Available online at www.sciencedirect.com
SCIENCE DIRECT®
Physica E 20 (2004) 196–203
PHYSICA E
www.elsevier.com/locate/physe

The 6.1 Å family (InAs, GaSb, AlSb) and its heterostructures: a selective review

Herbert Kroemer[a,b,*]

[a] *ECE Department, University of California, Santa Barbara, CA 93106, USA*
[b] *Materials Department, University of California, Santa Barbara, CA 93106, USA*

Abstract

The three semiconductors InAs, GaSb, and AlSb form an approximately lattice-matched set around 6.1 Å, covering a wide range of energy gaps and other properties. Of particular interest are heterostructures combining InAs with one or both of the antimonides, and they are emphasized in this review. In addition to their use in conventional device types (FETs, RTDs, etc.), several heterostructure configurations with unique properties have been explored, especially InAs/AlSb quantum wells and InAs/GaSb superlattices.

InAs/AlSb quantum wells are an ideal medium to study the low-temperature transport properties in InAs itself. With gate-induced electron sheet concentrations on the order 10^{12} cm^{-2}, they exhibit a pronounced conductivity quantization. The very deep wells (1.35 eV) provide excellent electron confinement, and also permit modulation doping up to at least 10^{13} electrons cm^{-2}. Because of the very low effective mass in InAs, heavily doped wells are essentially metals, with Fermi energies around 200 meV, and Fermi velocities exceeding 10^{8} cm s^{-1}. Contacted with superconducting electrodes, such structures can act as superconductive weak links.

InAs/GaSb-related superlattices with their broken-gap lineup behave like semimetals at large lattice periods, but if the lattice period is shortened, increasing quantization effects cause a transition to a narrow-gap semiconductor, making such structures of interest for infrared detectors, often combined with the deliberate addition of strain.

PACS: 73.20.−r; 73.21.−b; 73.40.Kp; 85.30.−z; 81.15.Hi; 85.60.Gz

Keywords: Heterostructures; Indium arsenide; Antimonides; Band lineup; Quantum wells; Superlattices; Infrared detectors

1. Introduction: band lineups

The three semiconductors InAs, GaSb, and AlSb form an approximately lattice-matched set around 6.1 Å, with (room temperature) energy gaps ranging from 0.36 eV (InAs) to 1.61 eV (AlSb). Like other compound semiconductors, they are of interest principally for their heterostructures, especially heterostructures combining InAs with the two antimonides and their alloys. This combination offers band lineups that are drastically different from those of the more widely studied (Al,Ga)As system, and the lineups are one of the principal reasons for interest in the 6.1 Å family. Such structures are emphasized in the present review. I will say nothing about heterojunctions involving just the two antimonides.

* ECE Department, University of California, Santa Barbara, CA 93106, USA. Tel.: +1-805-893-3078; fax: +1-805-893-7990.
E-mail address: kroemer@ece.ucsb.edu (H. Kroemer).

1386-9477/$ - see front matter © 2003 Elsevier B.V. All rights reserved.
doi:10.1016/j.physe.2003.08.003

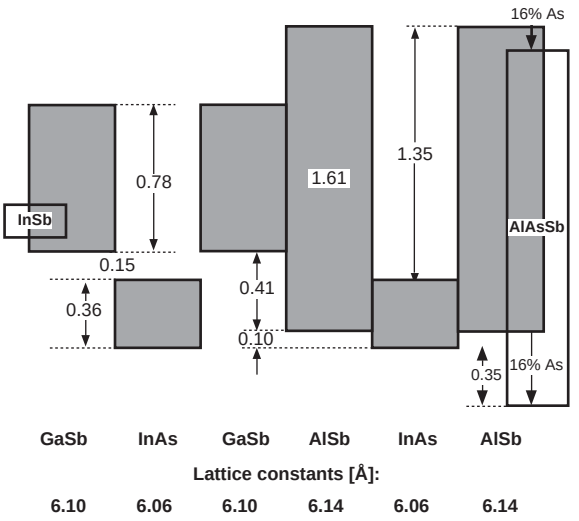

Fig. 1. Band lineups in the 6.1 Å family of semiconductors. The shaded areas represent the energy gaps. All energies are in eV. Adapted from Ref. [2], with additions of estimates for the lineups of InSb, and of Al(Sb,As) lattice-matched to InAs. For a recent comprehensive compilation of band parameters, see Ref. [3].

The most exotic lineup is that of InAs/GaSb heterojunctions, for which it was found already in 1977 by Sakaki et al. [1], that they exhibit a *broken gap* lineup: at the interface, the bottom of conduction band of InAs lines up *below* the top of the valence band of GaSb, with a break in the gap of about 150 meV (Fig. 1). It was probably this remarkable discovery that triggered much of the interest in the entire 6.1 Å family already early in the evolution of MBE technology.

The observation of a broken-gap lineup was not completely unexpected. In his 1977 pseudopotential theory of heterojunction band lineups, Frensley [4] had raised the likelihood of such a lineup. The Harrison LCAO theory of band lineups, also published in 1977 [5], yielded a similar prediction.

When replacing Ga with Al, the valence band drops by about 0.4 eV, closing the broken gap and leading to a weakly staggered lineup. At the same time, the conduction band rises by about 0.4 eV, leading to an exceptionally large InAs/AlSb conduction band offset of about 1.35 eV [6]. It makes possible very deep quantum wells and very high tunneling barriers, of great interest for both research and device applications.

Much of the work on heterostructures between InAs and the antimonides went beyond the use of *binary* AlSb or GaSb, going to ternary alloys like (Al,Ga)Sb, (Ga,In)Sb, or Al(Sb,As). The principal motivation for the use of (Al,Ga)Sb with about 10–20% of Ga—a substitution that actually reduces the lattice mismatch—is to enhance the chemical stability of AlSb against oxidation. An accompanying reduction in the large height of the electron barrier is largely inconsequential, but the accompanying reduction in the *residual gap* at the interface (the energy difference between the InAs conduction band and the AlSb valence band) can lead to leakage problems in gated structures.

Replacing some of the Sb atoms in AlSb by As atoms has the opposite effect: the energy gap increases, but the valence band drops by more than the energy gap increase, hence the conduction band actually drops in energy, eventually leading to a conventional straddling lineup [7]. Finally, if In is substituted for Ga, the energy gap narrows. Superlattices between InAs and either (Ga,In)Sb, or Al(Sb,As) are no longer lattice matched, but as long as the strain does not significantly exceed 1%, it does not necessarily lead to misfit dislocations in sufficiently thin layers. Instead, the strain leads to a reduction of the residual gap, a property utilized for long-wavelength infrared detectors, discussed in Section 6.

A final lineup property—of a different kind, but of great importance in all applications involving electron transport through InAs—concerns clean metal–InAs interfaces: the interface Fermi level is pinned at about 130 meV above the bottom of the conduction band [8]. Hence, metal–InAs contacts do not form electron-blocking Schottky barriers.

Given the limitations of space, the present review is necessarily incomplete, concentrating on selected aspects of heterostructures between InAs and (Al,Ga)As with varying Al:Ga ratio. Antimonide-only heterostructures are ignored, as are conventional devices, such as FETs and RTDs, in which the narrow gap of InAs plays only an incidental role. Additional details of some of the material presented here can be found in a longer 1999 review by Kroemer and Hu [2], but even there the coverage is by no means complete.

2. MBE growth

The MBE technology of both InAs and AlSb has been worked out to the point that the growth of such structures is now fairly routine. Following earlier

pioneering work of the IBM group of Chang et al., first on InAs/GaSb [9], and subsequently on InAs/AlSb [10], Tuttle et al. [11,12] started, in late-1985, to investigate the properties of InAs/AlSb quantum wells systematically and in considerable depth. As with other III–V semiconductors, RHEED observations and oscillations are important diagnostic tools, extensively studied by Subbanna et al. [13]. Subsequent contributions and further refinements were made by Nguyen et al. [14]. The reader interested in the MBE technology of these structures is referred to the papers cited.

An important "nuisance property" of GaSb and AlSb is that Si and Sn, the two preferred donors in the arsenides, are acceptors in GaSb and AlSb, which necessitates the use of column-VI elements as donors, like Te. Rather than using the element itself, we—and others—have found it preferable to follow an idea of McLean et al. [15], to use it in the form of a volatile compound, such as PbTe, which vaporizes as a PbTe molecule without dissociating, but splits up on the AlSb surface, with a significant fraction of the Te being incorporated into the growing crystal. The Pb, which has a fairly high vapor pressure, re-evaporates [16].

When the MBE growth is performed on lattice-mismatched GaAs substrates rather than on GaSb, the interposition of a proper buffer layer is essential for high-quality growth [14,17]. Using GaSb for the initial nucleation leads to very rough initial morphology. Nucleating with AlSb leads to much less initial surface roughness, but the residual roughness persists with continued growth, and leads to InAs quantum wells with poor transport properties. Following the initial thin AlSb nucleation layer with a thick (≈ 1 μm) GaSb buffer layer smoothes out the surface morphology, and if the growth is then switched to AlSb or (Al,Ga)Sb, the smooth surface persists, leading to InAs quantum wells with much better transport properties.

3. InSb-like versus AlAs-like interfaces

At InAs/(Al,Ga)Sb interfaces, both the cation and the anion change, in contrast to the common-anion (Al,Ga)As system. As a result, there are now two kinds of bond configurations possible: In–Sb bonds and Ga–As (or Al–As) bonds, the mix depending on growth details, and leading to a technology-dependent interface bond (and defect) configuration. The nature of the interface can be influenced by the shutter sequence during the crossover between the materials [12], with significant differences between "upper" and "lower" interfaces (i.e., above and below the InAs in the growth sequence), especially for AlAs-like interfaces. However, STM measurements show that the bond preferences at the interfaces are far from perfect [18].

The bonding type does not appear to influence the band offsets significantly, but Kroemer has speculated that at InSb-like interfaces some states are split off from the valence band and are moved as interface Tamm states into the residual gap, possibly even above the bottom of the InAs conduction band [19]. For now, this remains a hypothesis that has been neither confirmed nor refuted.

The In–Sb bonds are significantly longer and (Al,Ga)–As bonds significantly shorter than the bulk In–As and (Al,Ga)–Sb bonds. Hence, the interfaces are anisotropically strained. To a large extent that is a nuisance, but Fuchs et al. [20] have shown that in InAs/GaSb superlattices, strain compensation can be achieved by a controlled alternation between the two types. Other work of importance for the interface type problem is that by Spitzer et al. [21].

4. Doping and defects in the InAs/AlSb system

The doping properties of InAs–AlSb quantum wells are dominated by the fact that these wells are extraordinarily deep. Hence, even energetically very deep donors in the barrier will drain any available electrons into the well. Consequently, even not-intentionally doped wells tend to show relatively high electron sheet concentrations, on the order of 3×10^{11} electrons cm^{-2} and more. To understand the doping properties of these wells, (at least) three distinct sources of electrons must be considered: conventional shallow bulk donors, surface states, and deep donors at or near the hetero-interfaces.

4.1. Conventional shallow donors, and modulation doping

Because of the high barriers, very high electron concentrations are easily achieved by *modulation doping*,

i.e. placing the donors into the barriers rather than into the wells. The spatial separation of the ionized impurities from the electrons leads to reduced impurity scattering and hence to enhanced mobilities relative to bulk-doped wells. In this way, room temperature mobilities equal to the high-purity bulk limit of about $33,000\ \mathrm{cm^2\ V^{-1}\ s^{-1}}$ are readily achieved even for electron sheet concentrations around $1 \times 10^{12}\ \mathrm{cm^{-2}}$, corresponding to volume concentrations approaching $10^{18}\ \mathrm{cm^{-3}}$. Low-temperature mobilities approaching $1 \times 10^6\ \mathrm{cm^2\ V^{-1}\ s^{-1}}$ have also been achieved, at similar electron concentrations [22]. By increasing the doping levels further, much higher electron concentrations can be obtained, albeit at some loss in mobility [14].

4.2. Surface states as quantum well dopants

Because of the extreme depth of the quantum wells, reaching almost to the bottom of the energy gap of the AlSb barriers, surface states on the *outside* of the top barrier can be an important source of electrons inside the well. The effect depends strongly on the energetic location of the surface states, which in turn depends on the chemical nature of the surface coverage. Of particular interest has been the case of AlSb top barriers deliberately capped with a very thin layer of either GaSb or InAs to protect the AlSb against oxidation (Fig. 2).

The doping effect is most pronounced for wells with GaSb-capped top barriers, which exhibit a very high density of surface states ($\gg 10^{12}\ \mathrm{cm^{-2}}$) at an energy about 0.85 eV below the conduction band edge of the AlSb barrier [23]. Under flat-band conditions, that would be about 0.5 eV above the bottom of the InAs well. As a result, electrons from the surface states will drain into the well until the electric field introduced into the barrier by the charge transfer has pulled the surface state down to the same energy as the Fermi level inside the well [23]. The resulting charge transfer increases with decreasing barrier thickness. Controlled electron sheet concentrations in the range from about $3 \times 10^{11}\ \mathrm{cm^{-2}}$ to more than $1.5 \times 10^{12}\ \mathrm{cm^{-2}}$ have been achieved by a variation of the overall barrier thickness. In not-intentionally doped wells with sufficiently thin GaSb-capped top barriers, the electron concentrations in the wells are

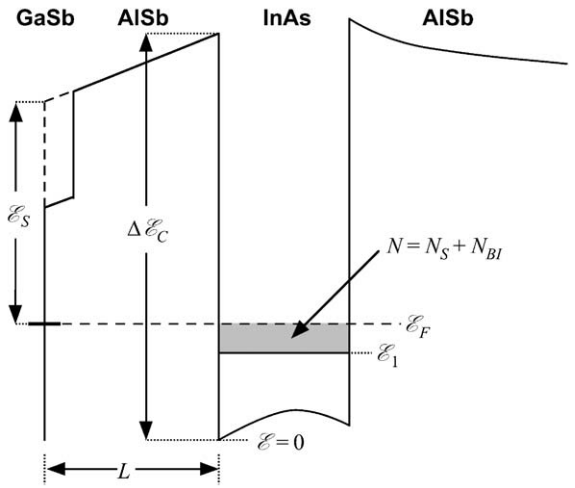

Fig. 2. Energy band diagram of a near-surface InAs/AlSb quantum well, with a potential drop across surface barrier, due to electron transfer from surface states to the quantum well. From Ref. [23].

dominated by electrons from surface states on the GaSb cap used to protect the AlSb.

The electron transfer is smallest if an InAs cap is used, corresponding to a surface pinning level at least 0.35 meV lower than on GaSb. The exact value depends on the chemical state of the InAs surface, including specifically on the degree of contamination, especially with Sb [24]. By working with multiple caps, like an InAs cap over a GaSb cap, and then selectively removing the upper cap, lateral structuring can be achieved [25].

4.3. Interface-related donors and defects

By using sufficiently thick top barriers and/or an InAs cap rather than a GaSb cap, electron sheet concentration down to $2–3 \times 10^{11}\ \mathrm{cm^{-2}}$ are readily achieved in not-intentionally doped wells.

These lower-limit concentrations are still much higher than what is obtainable in typical GaAs–(Al,Ga)As heterostructures, indicating the presence of an additional source of electrons. The concentrations are too high to be attributable to background donors in the InAs; the data call for a high concentration of donors either associated with the interface itself, or inside the barrier, but close to the interface. A quantitative analysis of the temperature dependence

of the residual electron concentrations [19] suggested a donor level less than 50 meV above the bottom of the *bulk* conduction band of InAs, which implies a level below the bottom of the quantum well, and below the Fermi level in the well at the observed electron concentrations. But in this case only a small fraction of the donors will be ionized, calling for a donor a concentration much higher than the observed electron concentrations, on the order of about 3×10^{12} donors cm^{-2} per well.

The nature of these donors is not clear. Kroemer proposed that they are not ordinary point defects, but are *Tamm states* at the InAs–AlSb interface [19], inherent to the band structure of that interface. Alternatively, Shen et al. [26] proposed that the donors are very deep bulk donor states associated with Al_{Sb} antisite defects, that is, Al atoms on Sb sites. With Al having two valence electrons less than Sb, one might naively expect that such defects would act as double acceptors, but the authors argue that in the vicinity of a quantum well that is even deeper than the energy levels associated with the antisites, the defects, rather than accepting one or two electrons from the AlSb valence band, can act as "false-valence" donors, by giving off one of their remaining electrons into the InAs well. The issue remains unresolved; evidently, more research on this crucial question is needed.

There is evidence for defects associated with the InAs/AlSb interface itself. Tuttle [12] found that *lower* interfaces of the AlAs type lead to very low mobilities and that they introduce a sheet of donor defects. Strong interface roughness and/or intermixing—definitely present at those interfaces (see, for example, Ref. [27])—could explain the low mobilities, but not the doping. Deep antisite donors of As atoms on Al sites, introduced during the interface switchover to As-stabilization, were invoked as an explanation, but that remains a hypothesis. Regardless of explanation, these observations have led to a widespread preference for InSb-like over AlAs-like interfaces. However, there is actually no evidence that *upper* AlAs interfaces lead to the same poor properties. In fact, the work by Fuchs et al. cited above shows that even in defect-sensitive IR detectors such interfaces do not degrade the performance.

There is some evidence for defects even at a presumably "good" InSb-like upper InAs/AlSb interface: In a study of AlSb/InAs/AlSb pnp heterostructure bipolar transistors, Pekarik et al. [28] found strong evidence for electron–hole pair recombination via interface defects rather than via near-interface bulk defects.

5. Electron mobilities in InAs/AlSb quantum wells

The electron mobilities in InAs/AlSb quantum wells depend strongly on both the well width and on the electron sheet concentration—not to mention "quality" issues. The dependence is strongest for the low-temperature ($\leqslant 10$ K) mobilities, which are a sensitive quality indicator.

Room-temperature mobilities in the range 30,000–33,000 $cm^2\ V^{-1}\ s^{-1}$, four times the value for GaAs, are routinely achieved in "good" modulation-doped InAs-AlSb quantum well samples with what appears to be an optimal combination of well width and electron sheet concentration (around 15 nm and 1.5×10^{12} cm^{-2}). In fact, in my judgment, mobilities below 30,000 $cm^2\ V^{-1}\ s^{-1}$ under these conditions indicate a flawed growth procedure.

For narrow wells ($\leqslant 10$ nm) the mobilities decrease steeply, with the inverse 6th power of the well width, due to interface roughness scattering [29,30]. As a result, widths below 15 nm are rarely used; the majority of studies have employed a 15 nm width, which appears to have become a de facto standard for transport studies in this system.

For wider wells, mobilities again decrease, albeit more slowly, due to the onset of inter-subband scattering; the exact point of onset depends on electron sheet concentrations. In a gated 15 nm structure in which the electron sheet concentration was varied by varying the gate voltage, Koester [31] found a low-temperature peak mobility of about 750,000 $cm^2\ V^{-1}\ s^{-1}$ at a sheet concentration of about 1.65×10^{12} cm^{-2}, dropping to about 300,000 $cm^2\ V^{-1}\ s^{-1}$ at about 2.25×10^{12} cm^{-2}. The highest low-temperature mobilities reported, 980,000 $cm^2\ V^{-1}\ s^{-1}$ at 4.2 K [22] and 944,000 $cm^2\ V^{-1}\ s^{-1}$ at 12 K [17], were obtained in wells with the above parameters.

The long mean free paths implied by the high peak mobilities lead to pronounced conductance quantization effects at low temperatures in ballistic constrictions of the current path in InAs/AlSb quantum if the constrictions are sufficiently narrow that they contain only a small but electronically variable number of

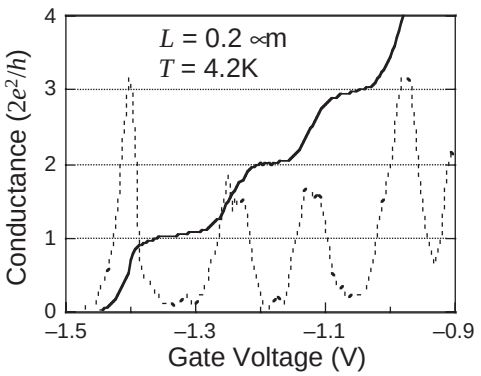

Fig. 3. Conductance quantization at 4.2 K in an InAs/AlSb constriction, created by a pair of reversed-biased gate electrodes applied to the device surface, with an electrode gap 120 nm wide and 200 nm long. The number of quantum channels remaining to participate in the conduction decreases with increasing reverse bias voltage applied to the electrodes, leading to quantized steps in the residual overall conductance (solid line). The broken line is the derivative of the solid line, in arbitrary units. Adapted from Ref. [32].

quantum channels (Fig. 3). It was shown by Koester [32] that the quantization persists up to constriction lengths approaching 2 μm, significantly exceeding the lengths possible with GaAs/(Al,Ga)As constrictions. A detailed review of this work is found in Ref. [2].

Remarkably high mobilities are still achievable even for much higher electron concentrations. For example, in two samples with electron sheet concentrations of 5.5×10^{12} and 6.9×10^{12} cm^{-2} mobilities as high as 220,000 and 196,000 cm^2 V^{-1} s^{-1} were obtained [33]. Such heavily doped wells are essentially metals, with Fermi energies around 200 meV (making allowance for strong non-parabolicity), and Fermi velocities exceeding 10^8 cm s^{-1}. Contacted with superconducting Nb electrodes, they act as superconductive weak links, a topic outside the scope of this review, but discussed extensively by Thomas et al. [34] and in the review of Ref. [2].

When the electron concentration is decreased below the optimal-mobility value, the Fermi velocity in the degenerate 2DEG decreases. This, in turn, increases impurity scattering, just as impurity scattering increases with decreasing temperature in a non-degenerate electron gas. In principle, in this low-concentration range, mobilities similar to those in GaAs should still be attainable in 15 nm wells, like values in excess of 10^6 cm^2 V^{-1} s^{-1} for electron concentrations far below 10^{12} cm^{-2}. However, in this range the mobilities in InAs/AlSb quantum wells tend to drop to values an order of magnitude or more below state-of-the-art GaAs values. We believe that these discrepancies are not of a fundamental nature, but simply reflect a state of the art for the new materials system which, while vastly improved over the last few years, is still far behind that for the more mature GaAs system. Presumably, the deep near-interface donors referred to above play an important role in limiting the mobility. Evidently, a lot of work remains to be done.

6. InAs/GaSb and InAs/(Ga,In)Sb broken-gap superlattices

Most of the applications of the 6.1 Å family to conventional devices, such as FETs and RTDs, do not explicitly draw on the narrow gap of InAs. They are therefore not discussed in the present review. The case of interest in the context of this conference is the use of the broken-gap alignment at InAs/GaSb interfaces to achieve effective energy gaps in InAs/GaSb-based superlattices that are narrower than that of InAs itself, down to zero. Such narrow gaps are of great interest for long-wavelength infrared applications, especially detectors, as potential competitors to devices based on HgCdTe.

At layer thicknesses large enough that quantum confinement effects are negligible, InAs/GaSb superlattices behave like semimetals, with the bottom of the InAs conduction band dipping below the top of the GaSb valence band. If the layer thicknesses are reduced, quantization effects push the lowest electron state in the InAs layers up, and the highest hole state in the GaSb layers down. Eventually, the electron states are pushed above the hole states, creating a narrow-gap semiconductor (Fig. 4). However, the following problem arises: The electrons are primarily located in the InAs and the holes in the GaSb, with wavefunction overlap mainly near the hetero-interfaces (see, for example, Ref. [35]). Because the optical absorption depends on this overlap, it is restricted to a vicinity of the interfaces, and for large SL layer thicknesses, much of the volume is optically inactive, leading to an undesirable reduction in the absorption. For a given

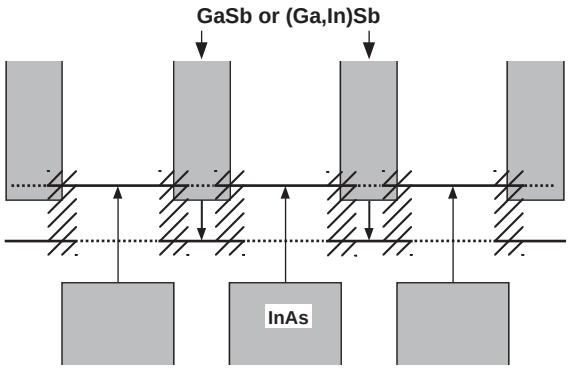

Fig. 4. Narrow-gap semiconductor created in a broken-gap InAs/GaSb or InAs/(Ga,In)As superlattice by quantum confinement. The arrows indicate the shifts in the lowest electron state and the highest hole state, forming a narrow SL gap. The electrons are largely located within the InAs and the holes in the GaSb; the broken-line portions of the SL band edges indicate regions where the relevant carriers have a small density, contributing only little to the absorption. The latter requires a wave function overlap, concentrated in the cross-hatched regions near the interfaces.

SL length, the latter is, to the first order, proportional to the number of interfaces rather than the nominal SL thickness.

As a result, for long-wavelength ($\lambda \geqslant 10$ μm) IR applications the primary problem is not the creation of an energy gap itself, but of a gap sufficiently *narrow* ($\leqslant 120$ meV)—which implies relatively weak quantum confinement—but at as short a lattice period as possible. The latter condition would of course favor strong quantization effects and large energy gaps, calling for a compromise between conflicting requirements. For a given SL period, the energy gap tends to decrease with a decreasing GaSb:InAs thickness ratio. Given a specified cutoff wavelength, that ratio should be chosen as low as possible compatible with the required energy gap. In a recent paper, Wei et al. have reported achieving cutoff wavelength beyond 25 μm in a SL with cells combining 16 InAs monolayers with 4 GaSb monolayers (an overall period of about 6.4 nm), with an interface bond configuration forced towards being pure InSb-like [36].

An additional degree of design freedom to optimize detector performance is the use of a *strained-layer superlattice* (SLS)—proposed already in 1987 by Smith and Mailhiot [37]—in which the GaSb has been replaced with (Ga,In)Sb, with up to 35% In. It was shown by these authors that the strain introduced by this substitution reduces the SL gap, or, conversely, that a desired gap can be reached at a shorter SL period, increasing the absorption. For a 1996 review of this topic, see Johnson et al. [38], who give detailed data on a SL designed for operation at 10 μm, composed of 3.9-nm-thick InAs layers and 1.6 nm-thick $Ga_{0.65}In_{0.35}Sb$ layers; they also include complete references to related earlier work. For some more recent progress, going beyond simple InAs/(Ga,In)Sb superlattices, and including applications beyond detectors, see Fuchs et al. [20]. For a cross-sectional STM image of a SLS, see Ref. [39].

References

[1] H. Sakaki, L.L. Chang, R. Ludeke, C.A. Chang, G.A. Sai-Halasz, L. Esaki, Appl. Phys. Lett. 31 (1977) 211.
[2] H. Kroemer, E. Hu, in: G.L. Timp (Ed.), Nanotechnology, Springer, Berlin 1999, p. 629.
[3] I. Vurgaftman, J.R. Meyer, L.-R. Ram-Mohan, J. Appl. Phys. 89 (2001) 5815.
[4] W.R. Frensley, H. Kroemer, Phys. Rev. B 16 (1977) 2642.
[5] W.A. Harrison, J. Vac. Sci. Technol. 14 (1977) 1016.
[6] A. Nakagawa, H. Kroemer, J.H. English, Appl. Phys. Lett. 54 (1989) 1893.
[7] S. Bhargava, H.-R. Blank, E. Hall, M. Chin, H. Kroemer, V. Narayanamurti, Appl. Phys. Lett. 74 (1999) 1135.
[8] S. Bhargava, H.-R. Blank, V. Narayanamurti, H. Kroemer, Appl. Phys. Lett. 70 (1997) 759.
[9] L.L. Chang, L. Esaki, Surf. Sci. 98 (1980) 70.
[10] C.-A. Chang, L.L. Chang, E.E. Mendez, M.S. Christie, L. Esaki, J. Vac. Sci. Technol. B 2 (1984) 214.
[11] G. Tuttle, H. Kroemer, J.H. English, J. Appl. Phys. 65 (1989) 5239.
[12] G. Tuttle, H. Kroemer, J.H. English, J. Appl. Phys. 67 (1990) 3032.
[13] S. Subbanna, J. Gaines, G. Tuttle, H. Kroemer, S. Chalmers, J.H. English, J. Vac. Sci. Technol. B 7 (1989) 289.
[14] C. Nguyen, B. Brar, C.R. Bolognesi, J.J. Pekarik, H. Kroemer, J.H. English, J. Electron. Mater. 22 (1993) 255.
[15] T.D. McLean, T.M. Kerr, D.I. Westwood, C.E.C. Wood, D.F. Howell, J. Vac. Sci. Technol. B 4 (1986) 601.
[16] S. Subbanna, G. Tuttle, H. Kroemer, J. Electron. Mater. 17 (1988) 297.
[17] M. Thomas, H.-R. Blank, K.C. Wong, H. Kroemer, J. Cryst. Growth 175/176 (1997) 849.
[18] J. Steinshnider, M. Weimer, R. Kaspi, G.W. Turner, Phys. Rev. Lett. 85 (2000) 2953.
[19] H. Kroemer, C. Nguyen, B. Brar, J. Vac. Sci. Technol. B 10 (1992) 1769.
[20] F. Fuchs, L. Burkle, R. Hamid, N. Herres, W. Pletschen, R.E. Sah, R. Kiefer, J. Schmitz, Proc. SPIE Photonics West 4288 (2001) 171.

[21] J. Spitzer, A. Höpner, M. Kuball, M. Cardona, B. Jenichen, H. Neuroth, B. Brar, H. Kroemer, J. Appl. Phys. 77 (1995) 811.
[22] C. Nguyen, Dissertation, UCSB, 1993.
[23] C. Nguyen, B. Brar, H. Kroemer, J.H. English, Appl. Phys. Lett. 60 (1992) 1854.
[24] C. Nguyen, B. Brar, H. Kroemer, J.H. English, J. Vac. Sci. Technol. B 11 (1993) 1706.
[25] C. Nguyen, B. Brar, V. Jayaraman, A. Lorke, H. Kroemer, Appl. Phys. Lett. 63 (1993) 2251.
[26] J. Shen, H. Goronkin, J.D. Dow, S.J. Ren, J. Appl. Phys. 77 (1995) 1576.
[27] B. Jenichen, S.A. Stepanov, B. Brar, H. Kroemer, J. Appl. Phys. 79 (1996) 120.
[28] J. Pekarik, H. Kroemer, J.H. English, J. Vac. Sci. Technol. B 10 (1992) 1032.
[29] C.R. Bolognesi, H. Kroemer, J.H. English, Appl. Phys. Lett. 61 (1992) 213.
[30] C.R. Bolognesi, H. Kroemer, J.H. English, J. Vac. Sci. Technol. B 10 (1992) 877.
[31] S.J. Koester, Dissertation, UCSB, 1995.
[32] S.J. Koester, B. Brar, C.R. Bolognesi, E.J. Caine, A. Patlach, E.L. Hu, H. Kroemer, M.J. Rooks, Phys. Rev. B 53 (1995) 13063.
[33] M. Thomas, R. Blank, personal communication.
[34] M. Thomas, H.-R. Blank, K.C. Wong, H. Kroemer, E. Hu, Phys. Rev. B 58 (1998) 11676.
[35] M.R. Kitchin, M. Jaros, Physica E 18 (2003) 498.
[36] Y. Wei, A. Gin, M. Razeghi, G.J. Brown, Appl. Phys. Lett. 81 (2002) 3675.
[37] D.L. Smith, C. Mailhiot, J. Appl. Phys. 62 (1987) 2545.
[38] J.L. Johnson, L.A. Samoska, A.C. Gossard, J.L. Merz, M.D. Jack, G.R. Chapman, B.A. Baumgratz, K. Kosai, S.M. Johnson, J. Appl. Phys. 80 (1996) 1116.
[39] J. Steinshnider, J. Harper, M. Weimer, C.H. Lin, S.S. Pei, D.H. Chow, Phys. Rev. Lett. 85 (2000) 4562.